Intensity duration frequency curve analysis for selected meteorological stations in North Shoa, Amhara Region, Ethiopia

Eyoel Yigletu Aybehon[*]

Dilla University, College of Engineering and Technology, Department of Water Resources and Irrigation Engineering, Dilla, Ethiopia

ABSTRACT

The estimation of rainfall intensity is required for the design of hydraulic and water resources engineering control structures. Rainfall data of 11 – 23 years long from four stations was used to generate Intensity-Duration-Frequency (IDF) curves and parameters for selected stations in the study area. The daily rainfall data set obtained was then subjected to frequency analysis to determine the distribution which best characterizes the data set. The result showed that Log Person Type III was the best fit probability distribution function. The annual extreme values of rainfall depth were computed for different rainfall durations and return periods. Ranked rainfall depths for each return period were converted to rainfall intensities. The corresponding rainfall intensities were computed for different rainfall durations and return periods. IDF curves were developed using MIDUSS 2.25 software for return periods of 2, 5, 10, 25, 50, and 100 years and for durations of 1, 2, 3, 6, 12, and 24 h, and determined IDF parameters. The results shown that for shorter durations (1 hour and 2 hours), the IDF curves gave higher intensities for the same return period while for longer durations (3 h, 6 h, 12 h and 24 h), they gave low intensities for the same return period. The IDF relationship developed can be used as valuable tool for the designing of hydraulic structures in the region. This study could serve as a spring board for other studies that imply the calculation of a peak flow and designing of hydraulic structures as an input to help improve flood resilience in the region.

INTRODUCTION

Rainfall intensity-duration-frequency curves are graphical representations of the intensity of rain that falls within a given period time. These curves are used to predict when an area will be flooded, or to pinpoint when a certain rainfall rate or

[*]Corresponding author: eyigeltu114@gmail.com

a specific volume of flow of runoff will reoccur in the future (DuPont and Allen, 2000).

In hydrologic risk analysis and design, quantifying extreme precipitation is an important factor. This will contribute in safe weather emergency planning, engineering structure design, reservoir management, and so forth. As a result, in hydrologic research, assessing excessive rainfall is crucial. A major means of this assessment is IDF analysis which is an empirical relationship between the rainfall intensity, duration and return period. It is a curve in which duration is taken as abscissa, intensity as ordinate and return period as third parameter. It has a variety of applications in land use planning, roads, soil conservation practices, sewer management, routing of storm water, etc.

The country is endowed with huge amount of water potential with annual surface water potential of 111 billion cubic meters and ground water potential of 2.6 billion cubic meters. The mean annual rainfall distribution has maxima (> 2000 mm) over the Southwestern highlands and minima < 300 mm) over the southeastern and northeastern lowlands (NMSA, 2001).

Many of structures constructed using the scarce financial resource and borrowed capital are not functioning as expected. A number of technical and management related factors could contribute to this under-performance of water resource development schemes. The technical performance is mainly due to lack of information for the design of structures. One of those design parameters needed but often not available is the rainfall IDF relationship. The result of this study will be useful to estimate the intensity and duration of an extreme rainfall event which is ultimately required for planning and design of water resource projects, flood control and flood plain mapping programs, urban drainage works, highway and culvert design, etc. Therefore, establishment of IDF curves and equations for the area is an important task for institutions and engineers involved in design and evaluation of water resource projects, highways, urban drainage works, etc., in the region.

IDF relationship curves are graphical representations of the amount of water that falls within a given period of time. This relationship is determined through statistical analysis of data from meteorological stations. The IDF presents excellent characteristics to make water resource project designs effective. As a result, the IDF technique has been used in many places. For instance, in eastern and northwest China, many researches were carried out to evaluate trends in extreme rainfall at different time scales over the past decade (Zhai *et al*., 2005; Zhu *et al*., 2018), in the Korean peninsula (Baek *et al*., 2016; Hua *et al*., 2018), in Japan (Kamiguchi *et al*., 2010), in India (Krishnamurthy *et al*., 2009), in the United States (Karl and Knight, 1998; Kunkel *et al*., 2013; US National Climate

Assessment, 2014) and in many other parts of the world (Alexander *et al*., 2006; Frich *et al*., 2002; Westra *et al*., 2013).

Change in climate due to industrialization has been identified as the major cause of global warming. The hydrological cycle has been changed due to the changes in the temperature and precipitation patterns. Climate models suggest that the probability of occurrence of intense rainfall in future will increase due to the increase in greenhouse gas emissions (Mailhot *et al*., 2010; Xu *et al*., 2018). Such changes in extreme events have enormous ecological, societal and economic impacts in the form of floods, droughts, heat waves, summer and ice storms and have great implications for municipalities.

Design standards at present are based on the historic climate information in the form of IDF curves required level of protection from natural phenomena (Koutsoyiannis *et al*., 1994; Koutsoyiannis *et al*., 1998). However, available information shows that North Shoa does not have IDF curves. The assessment, processing and presentation of data such as IDF need to have some standard or conventional form and should be simple for the users. Currently, since there are increases in number of rainfall records from recently installed recording rain gauges, it is possible to prepare IDF curves for different stations, regions and the country. The motivation to do this study stems from this opportunity and it was executed to establish the rainfall intensity-duration- frequency curves for North Shoa of the Amhara Region, Ethiopia.

MATERIALS AND METHODS

Description of the study area

The study was carried out in North Shoa which is one of 10 zones in Amhara Region, about 120 kilometers northeast of Addis Ababa on the paved high way to Dessie, the town has a latitude and longitude of 9°41′N 39°32′E/9.683°N 39.533°E/ and an elevation of 2,840 meters.

Data source

The data used for this study were recorded rainfall in hourly and daily basis obtained from the Ethiopian National Meteorological Agency (ENMA) from selected station. The selection criteria for the stations were being self-recording with having a relatively longer record time. As per the selection criteria, four stations were selected to prepare the desired data for IDF development (Table 1).
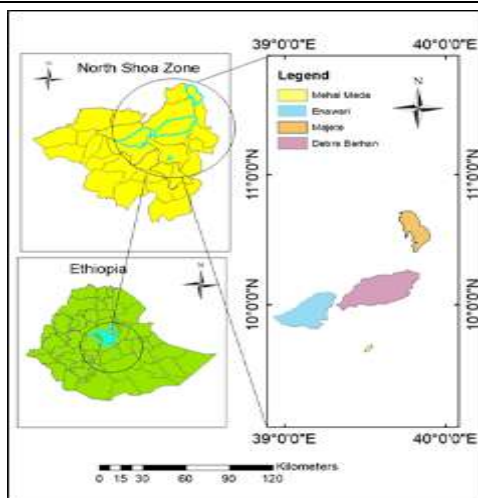
Figure 1. Location map of study stations in North Shoa

Table 1. Location and year of recording rain gauge station at the sites.

Station Name	Latitude (°N)	Longitude (°E)	Year of records
Debre Berhan	9.67	39.53	23
Enewari	9.83	39.15	11
Majete	10.4516	39.8487	11
Mehal Meda	10.23	39.68	20

Data processing and quality checking

Homogeneity test: - the homogeneity of all the series was checked by a non-parametric Mann-**K**endall rank test at 5% significance level.

Consistency analysis of the data set: - any inconsistency in the data set was checked and corrected using double mass-curve method.

Data analysis

Fitting the probability distribution

Literature review show that, Log Pearson Type III, Lognormal, and The Gumbel Extreme Value Type I were the three most appropriate Probability distribution used for IDF curves construction. In order to choose between the three distributions; the following steps were carried out:

For the purpose of comparison, the ranked annual maximum rainfall data sets of selected durations of 1, 2, 3, 6, 12, and 24 hours were fitted to Gumbel EVI, Log-

normal and Log-Pearson Type III frequency distributions and plots of annual maximum rainfall against these distributions were made. Finally, R-squared values for the given datasets revealed that Log Pearson Type III probability distribution relatively better describe the maximum annual rainfall values

Computation of extreme value (X_T)

The rainfall events X_T (mm) exceeding the observed value was estimated numerically using the following formula:

$$Y_T = \bar{Y} + K_T\, S_Y \rightarrow X_T = anti\log\left(\bar{Y} + K_T\, S_y\right) \tag{2.1}$$

Where Y_T is the reduced variate, y and S_y are the mean and standard deviation of the log transformed data, respectively. K_T is taken against the known value of skewness and desired return period. However, it can also be computed by using the following formula provided that the length of record must be infinite (Suresh, 2005).

$$K_T = \frac{\sqrt{6}}{\pi}\left[0.57721 + \ln\left(\ln\frac{T}{T-1}\right)\right] \tag{2.2}$$

Where T is the recurrence interval or return period.

Derivation of IDF equation

The IDF Curve Fit Software was used to solve the IDF parameters (a, b and c) values of an Intensity-Duration-Frequency equation of the general form

$$I = \left(\frac{a}{\left(t_d + b\right)^c}\right) \tag{2.3}$$

Where I is rainfall intensity (mm/hr), t_d is rainfall duration (minute), a is coefficient with the same unit as I, b is time constant (minute) and c is an exponent usually less than 1 (Cherkos Tefera, 2006).

IDF model performance evaluation

The IDF parameter estimation model was tested for its performance using the coefficient of determination (R^2) and the Nash and Sutcliffe simulation efficiencies (E_{NS}) values between the observed and estimated data sets. The coefficient of determination (R^2) formulae was checked the accuracy of the model output which is given by (Krause *et al.*, 2005) as:

$$R^2 = \left(\frac{\sum_{i=1}^{n} (O_i - \overline{O})(P_i - \overline{P})}{\sqrt{\sum_{i=1}^{n} (O_i - \overline{O})^2} \sqrt{\sum_{i=1}^{n} (P_i - \overline{P})^2}} \right) \qquad (2.4)$$

Where O_i observed and P_i predicted values.

$$E_{NS} = 1 - \frac{\sum_{i=1}^{n} (o_i - p_i)^2}{\sum_{i=1}^{n} (o_i - \overline{o})^2} \qquad (2.5)$$

where Oi and Pi = observed and predicted rainfall intensities; and O⁻ and P⁻ = means of the observed and predicted rainfall intensities at the respective durations, respectively.

The coefficient of determination, and the Nash and Suttcliffe (1970) simulation efficiency (E_{NS}) was checked according to the recommendation by Santhi *et al*. (2008) ($R^2 > 0.6$ and $E_{NS} > 0.5$).

Development of intensity duration frequency (IDF) models

Finally, the IDF curve was plotted on a Log Log scale, the duration D as abscissa and the intensity I as ordinate with the help of IDF curve fit tool curves for a given area based on the available data developed for various rainfalls to provide the design rain depths for various return periods and durations.

RESULTS AND DISCUSSION

Consistency and homogeneity analysis rainfall data

The graph of the double mass curve plot was found to be almost linear for all the considered stations with a coefficient of determination (R^2) ranging from 0.9952 to 0.9992 (Figure 2). This implies that the rainfall data were consistent over the considered period.
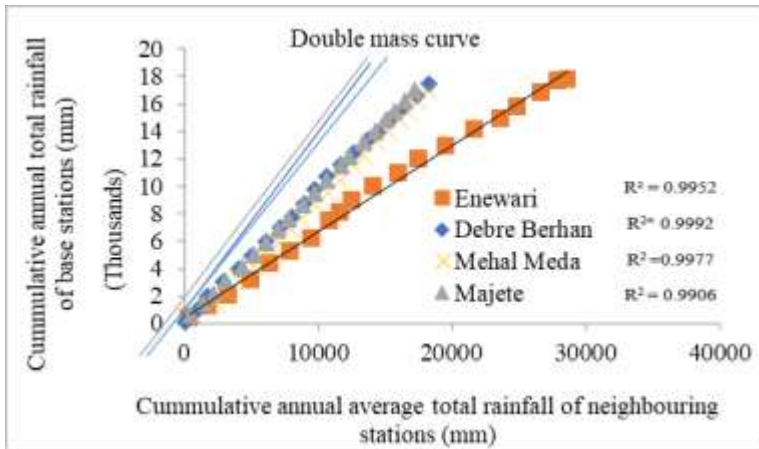
Figure 2. Double mass curves for consistency analysis of rainfall
data for the study areas.

The homogeneity and trend detections of the rainfall data series for each station
made by the Mann-Kendall test at the 5% significance level and its statistics are
summarized in Table 2. Based on the hypothesis, the computed p-values for the
stations of Deber Berhan, Mehal Meda, and Enewari were found to be greater
than the significance level ($\alpha = 0.05$); thus, one can detect that there is no trend in
the rainfall data series of these stations. This depicts that the data are
homogenous, independent, and identically distributed. However, a statistically
significant negative and positive trend was detected for Majete station.

Table 2. Summary statistics of the Mann-Kendal trend test (S) for the
considered stations.

Statistics	Enewari	Deber Berhan	Majete	Mehal Meda
Kendall's tau	-0.006	0.287	0.168	-0.193
(S)	-1.000	-49.00	32.000	-33.000
p-value (two-tailed)	1.000	0.255	0.516	0.448

Comparison and best-fitting of the probability distribution function

For comparison purpose, plot of maximum annual rainfall values for selected
durations (1, 2, 3, 6, 12 and 24 hours) were made against Gumbel EVI, log
normal and Log Pearson Type III probability distribution functions for Enewari

station (Figure 3). Appendix Figures 1 to 8 shows similar data for Majete, Deber Berhan and Mehal Meda stations.
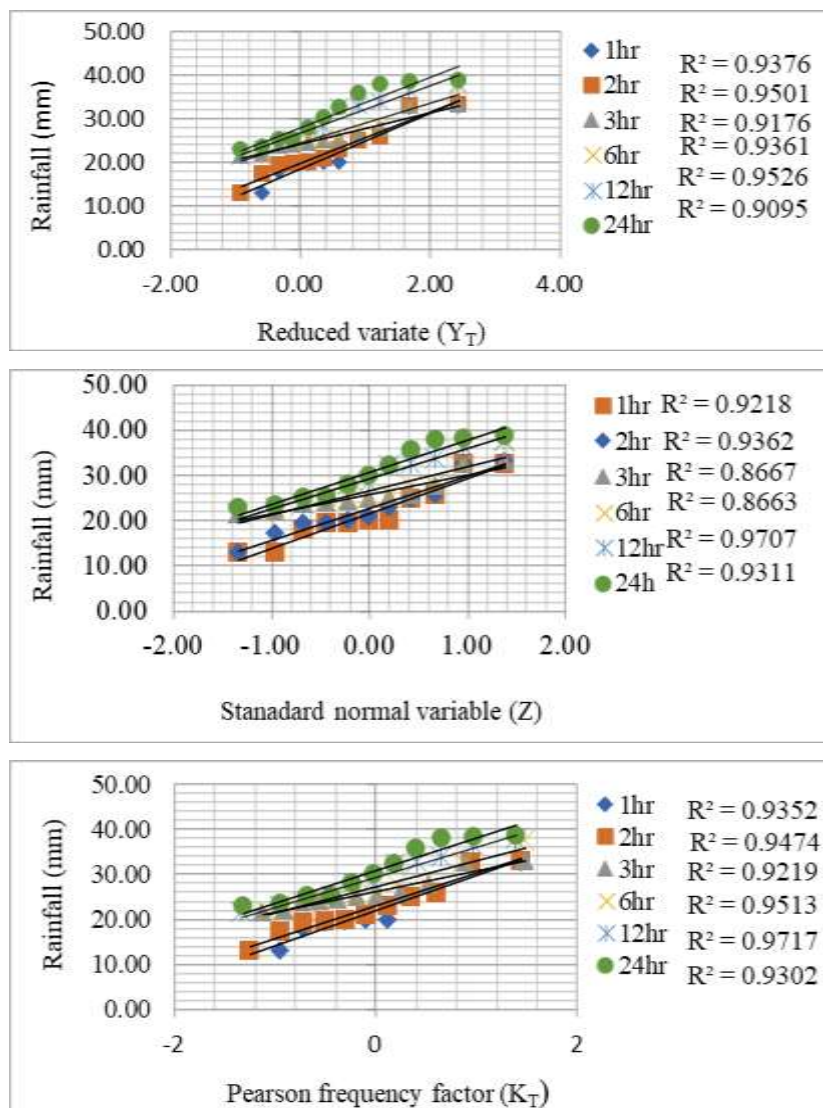
Figure 3. Top: Reduced variate (Y_T); Middle: Standard normal variable (Z); and Bottom: Pearson frequency factor (K_T) against the annual maximum rainfall at Enewari station.

IDF curves are obtained in order to estimate return periods by using a series of observed rainfall data with suitable distribution type according to the desired rainfall duration (Overeem *et al.*, 2008; Cheng *et al.,* 2014). There are methods which are mainly used theoretical distributions like Gumbel and Pearson Type 3 distributions that are applied in different regions of the world (Dupont and Allen, 2000; Nhat *et al.*, 2006; Acar and Senocak, 2008). Even though the Gumbel EVI distribution and Pearson Type 3 are suggested as the best-fitting distribution function around the world, the data series for the considered stations was also tested for Gumbel EVI, lognormal and log Pearson Type III distributions for more proof. The log Pearson Type III was found to be the most suitable probability distribution function for the data series of all the stations (Table 3).

Table 3. Calculated R^2 values of the probability distribution fitting test for all station.

Station name	Type of distribution	Coefficient of determination (R^2) values for indicated durations hr. (9 HR) (h)						Score	Rank
		1	2	3	6	12	24		
Enewari	Gumbel	0.937	0.950	0.917	0.936	0.952	0.909	-	-
	Log normal	0.921	0.936	0.866	0.866	0.970	0.931	-	-
	Log Pearson	0.935	0.947	0.921	0.951	0.971	0.930	-	-
	Score for G	3	3	2	2	1	1	12	2
	Score for LN	1	1	1	1	2	3	9	3
	Score for LP	2	2	3	3	3	2	15	1
Debr Berhan	Gumbel	0.954	0.959	0.968	0.969	0.960	0.948	-	-
	Log normal	0.916	0.930	0.941	0.952	0.960	0.959	-	-
	Log Pearson	0.955	0.959	0.965	0.963	0.961	0.958	-	-
	Score for G	2	3	3	3	2	1	14	3
	Score for LN	1	1	1	1	1	3	8	2
	Score for LP	3	2	2	2	3	2	14	1
Majete	Gumbel	0.959	0.978	0.970	0.970	0.933	0.885	-	-
	Log normal	0.978	0.984	0.985	0.986	0.969	0.942	-	-
	Log Pearson	0.978	0.986	0.985	0.986	0.972	0.959	-	-
	Score for G	1	1	1	1	1	1	6	3
	Score for LN	2	2	2	2	2	2	12	2
	Score for LP	3	3	3	3	3	3	18	1
Mehal Meda	Gumbel	0.969	0.934	0.942	0.906	0.885	0.905	-	-
	Log normal	0.963	0.961	0.971	0.945	0.942	0.959	-	-
	Log Pearson	0.974	0.960	0.972	0.946	0.949	0.965	-	-
	Score for G	2	1	1	1	1	1	7	3
	Score for LN	1	3	2	2	2	2	12	2
	Score for LP	3	2	3	3	3	3	17	1

Note: G = Gumbel; LN = lognormal; and LP = log Pearson distribution functions; and the values 3, 2, and 1 represent high, medium, and low marks.

The R-squared values for the given data sets showed that Log Pearson Type III probability distribution better described the maximum annual rainfall values (Table 3). Hence, for any required frequencies exceeding the number of observations can be extrapolated from the graphs analyzed by Log Pearson Type III probability distribution.

Estimation of IDF parameters and formulate mathematical equations

The estimation of IDF parameters A, B and C were done using the IDF curve fit software (MIDUSS Version 2.25) (Table 4). A general trend of the data was observed in A, B and C parameters. The "A" coefficient increased with an increase in return period and also the duration of rainfall for all of the stations. The "B" constantly decreased with an increasing return period for all station. Exceptionally, the "C" exponent generally increased or decreased with increasing recurrence interval for all stations which is in line with Yohannes (2017).

Table 4. Values of IDF Parameter for different return periods (value of each parameter for each return period).

RP (Year)		2	5	10	25	50	100
Enewari	A	1010.1	1048.7	127.6	1608.20	1920.87	229.00
	B	9.1	0.1	0.1	0.02	0.023	0.01
	C	0.9	0.9	0.9	0.90	0.9	0.96
Debre Berhan	A	1154.4	1519.3	1861.7	2403.72	3138.36	4114.49
	B	14.1	7.6	4.4	0.47	0.2	0.14
	C	1.0	1.0	1.0	0.90	1.0	1.00
Majete	A	1249.4	1801.2	2281.4	3055.85	358.07	4422.90
	B	29.0	25.8	24.2	20.56	17.03	14.07
	C	1.0	1.0	1.0	0.99	0.98	0.98
Mehal Meda	A	722.0	807.3	878.0	880.10	945.50	1011.76
	B	40.7	36.9	32.3	29.03	29.03	29.02
	C	0.8	0.8	0.8	0.78	0.79	0.79

Mathematical IDF expressions were developed for all stations using the estimated IDF parameters for a given duration and frequency taking the IDF model proposed by:

$$I = \frac{a}{(T_d + b)^C}$$

Where, "I" is rainfall intensity (mm/hr), A, B and C are the estimated IDF parameters and D is rainfall duration in minutes (Table 5).

The IDF formulas are the empirical equations representing a relationship among maximum rainfall intensity, rainfall duration and frequency. The general formula

for the study area to determine rainfall intensity for different return period is formulated as shown in Table 5.

Table 5. Mathematical IDF equations for the considered stations at different return periods.

Station	Return (Year)	Equation of rainfall intensity for each return period
Enewari	2	$I = \dfrac{1010.96}{\left(T_d + 9.098\right)^{0.9183}}$
	5	$I = \dfrac{1048.67}{\left(T_d + 0.054\right)^{0.9027}}$
	10	$I = \dfrac{1267.56}{\left(T_d + 0.056\right)^{0..9162}}$
	25	$I = \dfrac{1608.19}{\left(T_d + 0.0178\right)^{0.9330}}$
	50	$I = \dfrac{1920.87}{\left(T_d + 0.0233\right)^{0..9457}}$
	100	$I = \dfrac{2290.11}{\left(T_d + 0.008\right)^{0.9582}}$
Debre Berhan	2	$I = \dfrac{1154.37}{\left(T_d + 14.069\right)^{0.9455}}$
	5	$I = \dfrac{1519.30}{\left(T_d + 7.623\right)^{0.9469}}$
	10	$I = \dfrac{1861.71}{\left(T_d + 4.381\right)^{0.9508}}$
	25	$I = \dfrac{2403.72}{\left(T_d + 0.472\right)^{0.9557}}$

	50	$$I = \frac{3138.36}{(T_d + 0.2016)^{0.9703}}$$
	100	$$I = \frac{4117.49}{(T_d + 0.137)^{0.9858}}$$
Majete	2	$$I = \frac{722.07}{(T_d + 40.742)^{0.7603}}$$
	5	$$I = \frac{807.27}{(T_d + 36.889)^{0.7780}}$$
	10	$$I = \frac{877.99}{(T_d + 32.270)^{0.7879}}$$
	25	$$I = \frac{880.16}{(T_d + 29.035)^{0.7834}}$$
	50	$$I = \frac{945.50}{(T_d + 29.034)^{0.7883}}$$
	100	$$I = \frac{1011.76}{(T_d + 29.021)^{0.7929}}$$
Mehal Meda	2	$$I = \frac{1249.38}{(T_d + 28.966)^{0.9752}}$$
	5	
	10	$$I = \frac{1801.26}{(T_d + 25.815)^{0.9812}}$$
		$$I = \frac{2281.44}{(T_d + 9.098)^{0.9183}}$$
	25	$$I = \frac{3055.85}{(T_d + 20.5628)^{0.9874}}$$
	50	$$I = \frac{3658.07}{(T_d + 17.034)^{0.9844}}$$

100

$$I = \frac{4422.90}{\left(T_d + 14.068\right)^{0.983}}$$

Test for model performance

The values of coefficients of determination and Nash and Sutcliff simulation showed that almost all values are very close to 1 (Tables 6 - 10). Therefore, there were good direct correlations between observed and computed observations. Hence, it could be said that the computed intensity values obtained by using the IDF coefficients would adequately describe the observed data and the parameter estimation model performs very well. Therefore, using the computed rainfall intensity values of different durations and return periods, the IDF curves for selected stations can be constructed.

Table 6. Values of the coefficients of determination (R^2) and Nash and Sutcliff simulation (ENS) for different return period for Enewari station.

Return period (yr.)	Observed rainfall intensity (mm/hr.)						R^2	ENS
2	20.86	11.18	8.55	4.37	2.41	1.25		
5	26.76	13.59	9.62	5.03	2.82	1.49		
10	31.90	15.40	10.41	5.51	3.13	1.66		
25	38.87	18.20	11.49	6.19	3.56	1.92		
50	45.57	20.54	12.36	6.75	3.92	2.13		
100	52.89	23.17	13.29	7.36	4.32	2.37		
	Model predicted rainfall intensity (mm/hr.)							
2	20.68	11.65	8.2	4.4	2.38	1.26	0.9996	0.9719
5	26.01	13.92	9.65	5.16	2.76	1.48	0.9991	0.9956
10	29.75	15.77	10.88	5.77	3.06	1.2	0.9974	0.9995
25	35.25	18.46	12.65	6.62	3.47	1.82	0.9939	0.9998
50	39.97	20.75	14.15	7.34	3.81	1.98	0.9905	0.9999
100	45.29	23.31	15.81	8.14	4.19	2.16	0.9869	0.9999

Table 6. Values of the coefficients of determination (R^2) and Nash and Sutcliff simulation (E_{NS}) for different return period for Debr Berhan station.

Return period (y)	2	5	10	25	50	100
Observed rainfall	19.73	28.18	35.8	48.07	59.97	74.9
intensity (mm/hr.)	11.23	15.3	18.77	24.32	29.47	35.65
	7.92	10.72	13.09	16.85	20.32	24.48
	4.26	5.65	6.81	8.63	10.29	12.24
	2.26	2.97	3.57	4.5	5.34	6.32
	1.18	1.54	1.84	2.3	2.71	3.2
Model predicted	19.71	28.1	35.48	47.68	58.87	75.52
rainfall intensity	11.24	15.4	18.97	24.68	30.1	36.66
(mm/hr.)	7.93	10.69	13.05	16.77	20.32	24.59
	4.26	5.65	6.83	8.66	10.38	12.42
	2.25	2.96	3.55	4.47	5.3	6.27
	1.18	1.54	1.84	2.3	2.7	3.17
R^2	0.9996	0.9991	0.9974	0.9939	0.9905	0.9869
ENS	0.9719	0.9956	0.9995	0.9998	0.9999	0.9999

Table 8. Values of the coefficients of determination (R^2) and Nash and Sutcliff simulation (E_{NS}) for different return period for Majete station.

Return period (yr.)	2	5	10	25	50	100
Observed	21.88	23.27	25.71	26.29	27.67	29.04
rainfall	14.77	15.39	16.33	17.04	17.86	18.68
intensity l	12.00	12.34	12.95	13.49	14.11	14.72
(mm/hr.)	7.71	7.80	8.07	8.38	8.74	9.09
	4.64	4.64	4.75	4.92	5.12	5.31
	2.79	2.75	2.79	2.89	3.00	3.10
Model	21.65	23.00	24.84	26.13	27.47	28.80
predicted	15.18	15.81	16.74	17.45	18.30	19.14
rainfall	11.93	12.29	12.89	13.39	14.02	14.64
intensity	7.58	7.68	7.94	8.23	8.59	8.94
(mm/hr.)	4.66	4.65	4.76	4.93	5.13	5.32
	2.81	2.76	2.80	2.91	3.01	3.12
R^2	0.9996	0.9991	0.9974	0.9939	0.9905	0.9869
ENS	0.9719	0.9956	0.9995	0.9998	0.9999	0.9999

IDF Curve for the Stations

IDF curves were plotted for different durations and return periods for stations under study (Figures 4 – 7). These figures explain why larger hydrological structures such as dams and bridges are designed for higher return periods while small hydrological structures such as culverts and drainage gutters are designed for low return periods. Also, for a given return period, rainfall intensities decrease

with increase in duration. This implies that high intensity rainfall of short duration could have high devastating consequences of runoff to the environment.

Table 9. Values of the coefficients of determination (R^2) and Nash and Sutcliff simulation (E_{NS}) for different return period for Mahel Meda station.

Return period (yr.)	2	5	10	25	50	100
Observed rainfall intensity (mm/hr.)	15.70	22.90	29.10	40.32	50.97	64.31
	9.46	13.47	17.01	22.85	28.44	35.35
	6.86	9.74	12.29	16.49	20.50	25.45
	3.66	5.17	6.49	8.66	10.72	13.24
	2.03	2.77	3.40	4.41	5.35	6.48
	1.00	1.40	1.75	2.32	2.86	3.51
Model predicted rainfall intensity (mm/hr.)	15.70	22.83	29.08	40.09	50.82	64.25
	9.50	13.57	17.12	23.14	28.83	35.86
	6.83	9.68	12.16	16.29	20.16	24.93
	3.72	5.22	6.53	8.65	10.64	13.08
	1.97	2.74	3.41	4.49	5.50	6.74
	1.02	1.41	1.75	2.29	2.81	3.44
R^2	0.9996	0.9991	0.9974	0.9939	0.9905	0.9869
E_{NS}	0.9719	0.9956	0.9995	0.9998	0.9999	0.9999

CONCLUSION

The estimation of rainfall intensity is commonly required for the design of hydraulic and water resources engineering control structures. Various distribution functions were used for analysis and coefficient of determination (r^2) were used to identify the best probability distribution function. based on the coefficient of determination (r^2) among the three common probability distribution functions (i.e., Log normal, Log Person Type III and Gumbel EVI), Log Person Type III probability distribution was found to be the best function to fit the historical or observed data in the study area. The IDF curve fit parameters (A, B and C) generated with software known as MIDUSS Version 2.25 showed no specific tendency of increase or decrease with return periods. The probable reason for this could be that the software used to estimate the parameters has no provision to constrain the range of the values used to fit the model. Generally, the parameters varied from 722.1 to 4422.9 for a, 0.01 to 40.7 for b and 0.76 to 0.99 for parameter c. The values of observed intensities and computed intensities obtained by computer program were correlated by determining the coefficient of determination (R^2) and Nash and Sutcliffe simulation efficiency (E_{NS}). Since

these coefficients were very high (> 0.99), there was a strong relation between the observed and computed intensities. The IDF curves developed and the IDF parameters generated for the return periods of 2, 5, 10, 25, 50 and 100 years and for rainfall durations of 1, 2, 3, 6, 12 and 24 hours were good to use for water resource designing, soil and water conservation practices, etc. The plots were generally good to use for return periods of 2 years to 100 years and durations of 1 hour to 24 hours for the study area.
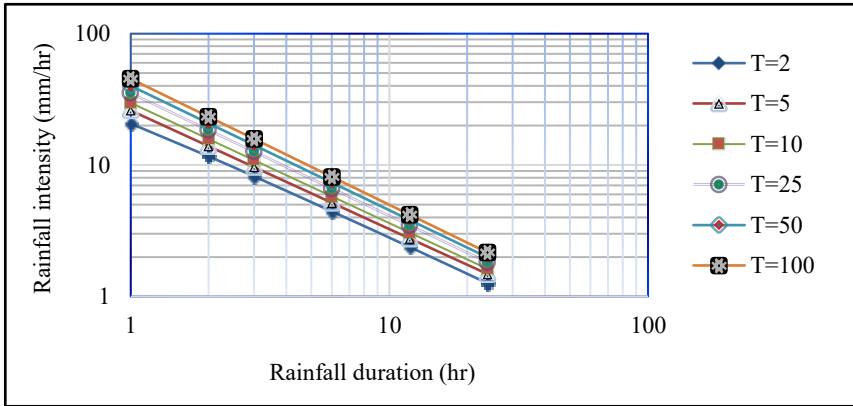
Figure 4. IDF curve for Enewari station.
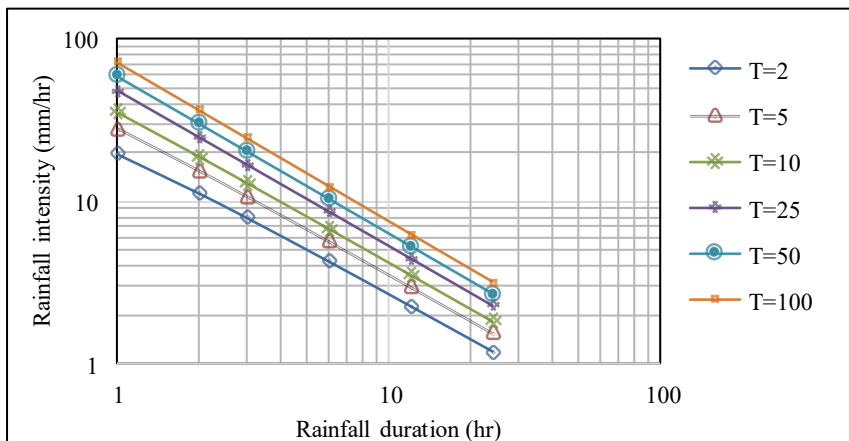
Figure 5. IDF curve for Debre Berhan station.
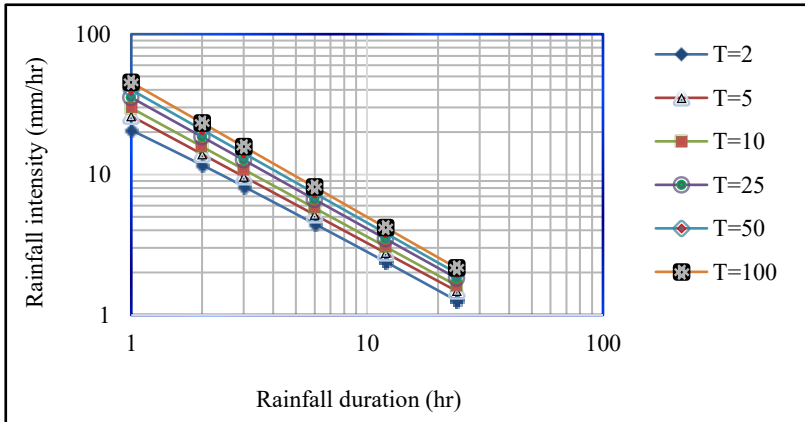
Figure 6. IDF curve for Majete station
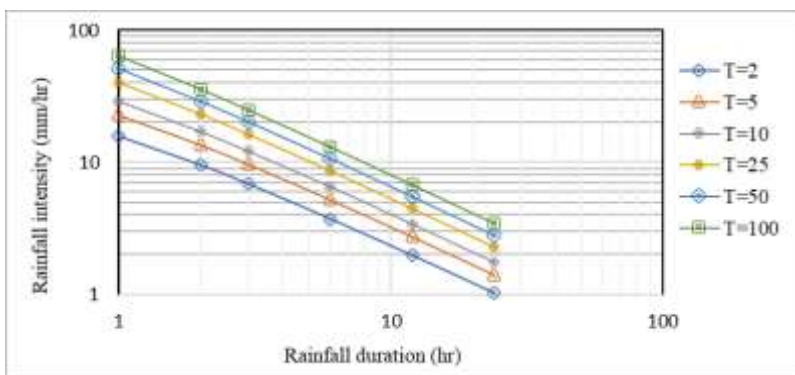
Figure 7. IDF curves for Mehal Meda station.

ACKNOWLEDGMENTS

Competing interests

The authors declare that they have no competing interests.

Ethical statement

I, Eyoel Yigletu, consciously assure that this material is my own original work, which has not been published before.

REFERENCES

Acar, R and Senocak, S. (2008). Modelling of short duration rainfall intensity equations for Ankara, Turkey, BALWOIS 2008-Ohrid, Republic of Macedonia-27.

Alexander, L., Zhang, X., Peterson, T., Caesar, J., Gleason, B., Klein Tank, A., Haylock, M., Collins, D., Trewin, B and Rahimzadeh, F. (2006). Global observed changes in daily climate extremes of temperature, climate a precipitation. *Journal of Geophysical Research: Atmospheres* **111** (D5).

Baek, H.J., Kim, M.K and Kwon, W.T. (2016). Observed short-and long-term changes in summer precipitation over South Korea and their links to large-scale circulation anomalies. *International Journal of Climatology*. DOI: 10.1002/joc.4753

Cheng, A., AghaKouchak, E and Gilleland, R.W. (2014) Non-stationary extreme value analysis in a changing climate. *Climate Change* **127**(4): 353–369.

Cherkos Tefera (2010). Rainfall intensity-duration-frequency relationship for Northern Ethiopia 23: Zede Journal 29-38.

DuPont, B.S and Allen, D.L. (2000). Revision of the Rainfall- Intensity Duration curves for the Common Wealth of Kentucky. Kentucky Transportation Center Research Report, Report Number: KTC-00-18/SPR-178-98. DOI: http://dx.doi.org/10.13023/KTC.RR.2000.18

Frich, P., Alexander. L.V., Della-Marta, P., Gleason, B., Haylock, M., Klein Tank, A.M.G and Peterson, T. (2002). Observed coherent changes in climatic extremes during the second half of the twentieth century. *Climate Research* **19**: 193-212. doi:10.3354/cr019193

Hua, L., Jiang, Y., Li, H and Zhou, X.Y. (2018). Hydraulic performance of low-pressure sprinkler with special-shaped nozzles. *Journal of Drainage and Irrigation Machinery Engineering* **36**(11): 1109–1114.

Kamiguchi, K., Arakawa, O., Kitoh, A., Yatagai, A., Hamada, A and Yasutomi, N. (2010). Development of APHROJP, the first Japanese high-resolution daily precipitation product for more than 100 years. *Hydrological Research Letters* **4**: 60–64.

Karl, T.R and Knight, R.W. (1998). Secular trends of precipitation amount, frequency, and intensity in the United States. *Bulletin of American Meteorological Society* **79**(2): 231–241.

Koutsoyiannis, D. (1994). A stochastic disaggregation method for design storm and flood synthesis. *Journal of Hydrology* **156**(1): 193–225. DOI: 10.1016/0022-1694(94)90078-7

Koutsoyiannis, D., Kozonis, D and Manetas, A. (1998). A mathematical frame work for studying rainfall intensity-duration- frequency relationships. *Journal of Hydrology* **206**((1-2): 118–135.

Krause, P., Boyle, D.P and Bäse, F. (2005). Comparison of different efficiency criteria for hydrological model assessment. *Advances in Geosciences* **5**: 89–97. https://doi.org/10.5194/adgeo-5-89-2005

Krishnamurthy, C.K.B., Lall, U and Kwon, H. (2009). Changing frequency and intensity of rainfall extremes over India from 1951 to 2003. *Journal of Climate* **22**(18): 4737–4746.

Kunkel, K.E., Karl, T.R., Brooks, H., Kossin, J., Lawrimore, J.H., Arndt, D., Bosart, L., Changnon, D., Cutter, S.L and Doesken, N. (2013). Monitoring and understanding trends in extreme storms: State of knowledge. *Bulletin of American Meteorological Society* **94**(4): 499–514.

Mailhot, A., Duchesne, S., Caya, D and Talbot, G. (2010). Assessment of future change in intensity-duration-frequency curves for Southern Quebec using the Canadian Regional Climate Model. *Journal of Hydrology* **347**(1-2): 197–210. DOI: 10.1016/j.jhydrol.2007.09.019

Nash, J.E and Sutcliffe, J.V. (1970). River flow forecasting through conceptual models part I – A discussion of principles. *Journal of Hydrology* **10**(3): 282–290. https://doi.org/10.1016/0022-1694(70)90255-6

Nhat, M.L., Tachikawa, Y and Takara, K. (2006). Derivation of rainfall intensity-duration frequency relationships for short-duration rainfall from daily data. disaster prevention Research Institute, Kyoto University, Uji, Kyoto 611-0011, Japan.

NMSA (National Meteorological Service Agency). (2001). Assessment of drought in Ethiopia. No.2. Addis Ababa, Ethiopia.

Overeem, A., Buishand, A and Holleman, I. (2008). Rainfall depth-duration-frequency curves and their uncertainties *Journal of Hydrology* **348:** 124–134.

Santhi, C., Kannan, N., Arnold, J.G and Di Luzio, M. (2008). Spatial calibration and temporal validation of flow for regional-scale hydrologic modeling. *Journal of American Water Resources Association* **44**(4): 829–846.

Suresh, R. (2005). Watershed hydrology: Principles of hydrology. Standard Publishers Distributors: New Delhi, India.

US National Climate Assessment (2014). Climate change impacts in the United States. The Third National Climate Assessment. http://nca2014.globalchange.gov/

Westra, S., Alexander, L.V and Zwiers, F.W. (2013). Global increasing trends in annual maximum daily precipitation. *Journal of Climate* **26**(11): 3904–3918.

Xu, S.R., Wang, X.K., Xiao, S.Q., Fan, E.D., Zhang, C.X., Xue, Z.L and Wang, X. (2018). Experimental study on double-nozzle jet sprinkler. *Journal of Drainage and Irrigation Machinery Engineering* **36**(10): 981–984.

Yohannes Gerezihier Gebremedhin (2017). Development of rainfall intensity-duration frequency (IDF) relationships for Siti zone, in case of Ethiopia Somali Regional State. *Civil and Environmental Research* **9**(8): 10–28.

Zhai, P., Zhang, X., Wan, H and Pan, X. (2005). Trends in total precipitation and frequency of daily precipitation extremes over China. *Journal of Climate* **18**(7): 1096–1108.

Zhu X.Y, Chikangaise, P., Shi., W.D., Chen W. H and Yuan S. Q. (2018). Review of intelligent sprinkler irrigation technologies for remote autonomous system. *International Journal of Agricultural and Biological Engineering* **11**(1): 23–30.

Appendices
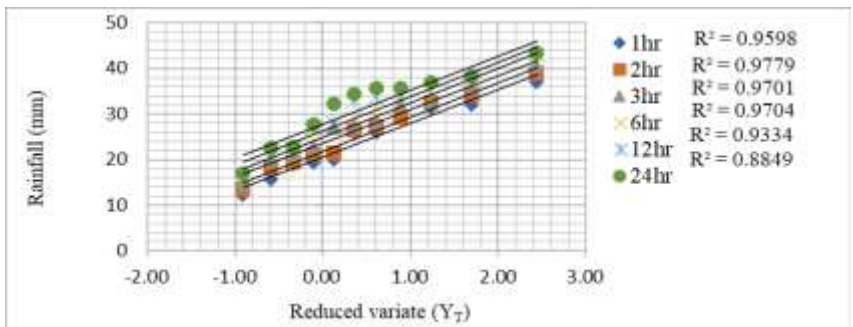
Appendix Figure 1. Plot of reduced vitiate (YT) against annual maximum rainfall for Gumbel probability distribution for Majete station
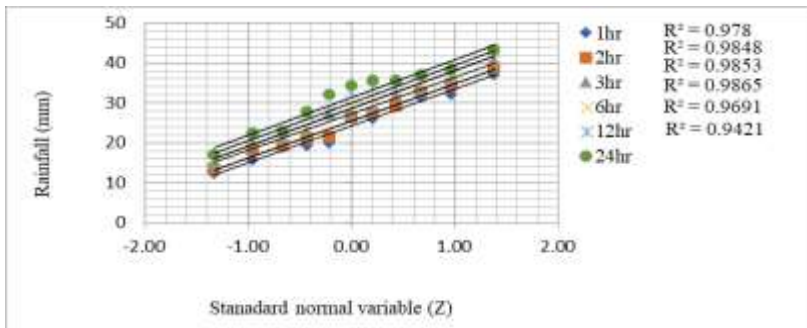
Appendix Figure 2. Plot of standard normal variable against annual maximum rainfall for log normal probability distribution for Majete station.
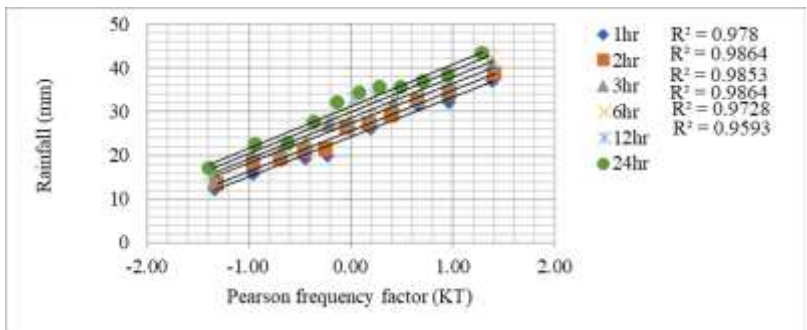
Appendix Figure 3. Plot of Pearson frequency factor against annual maximum rainfall for log Pearson probability distribution for Majete station.
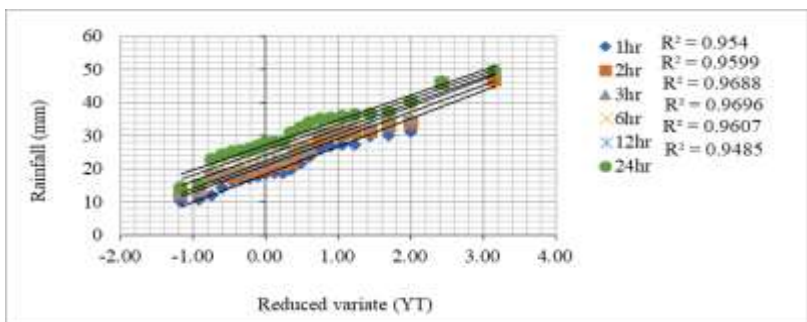
Appendix Figure 4. Plot of reduced variate (YT) against annual maximum rainfall for Gumbel probability distribution for Debre Berhan station.
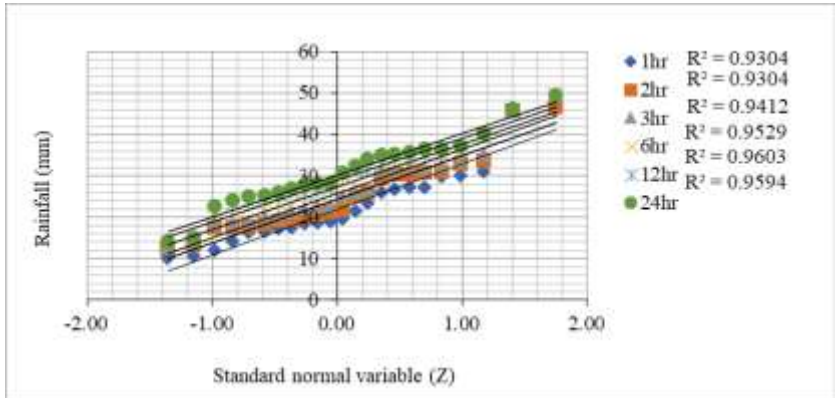
Appendix Figure 5. Plot of Standard normal variable against annual maximum rainfall for log normal probability distribution for Debre Berhan station.
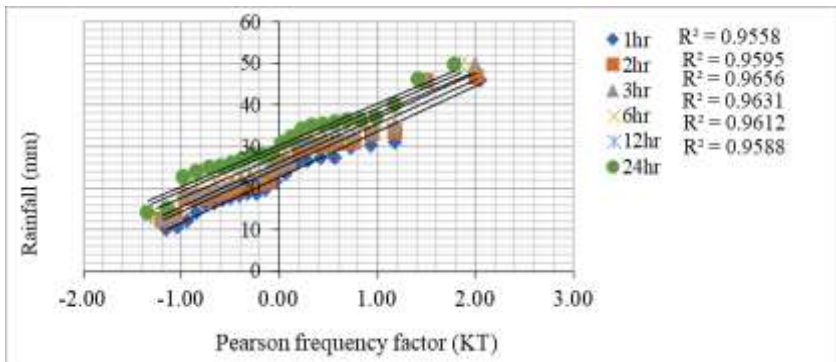
Appendix Figure 6. Plot of Pearson frequency factor against annual maximum rainfall for log Pearson probability distribution for Debre Berhan station.
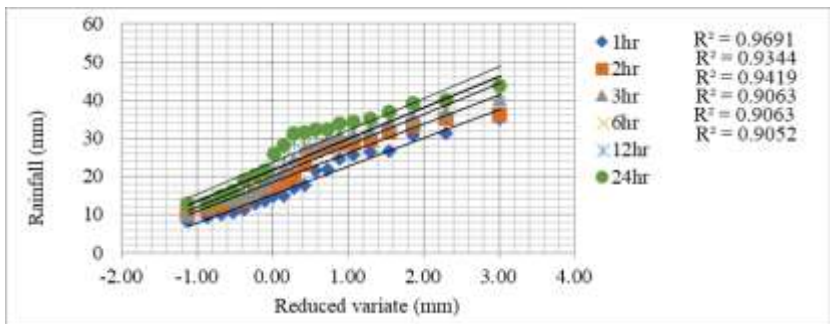
Appendix Figure 7. Plot of reduced variate (YT) against annual maximum rainfall for Gumbel Pearson probability
distribution for Mehal Meda station.
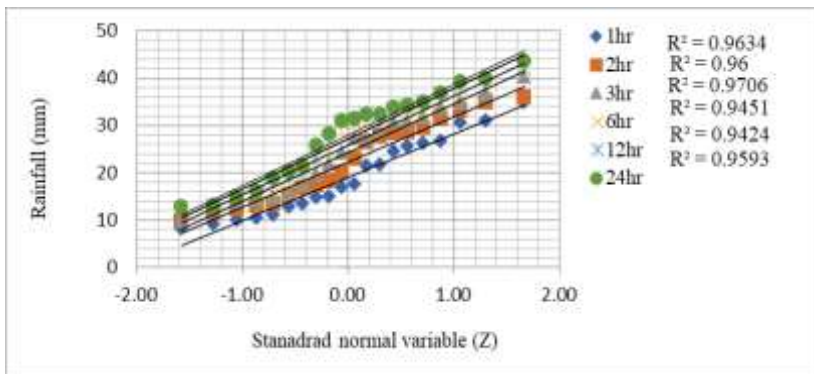
Appendix Figure 8. Plot of Standard normal variable against annual maximum rainfall for log normal probability distribution for Mehal Meda station.
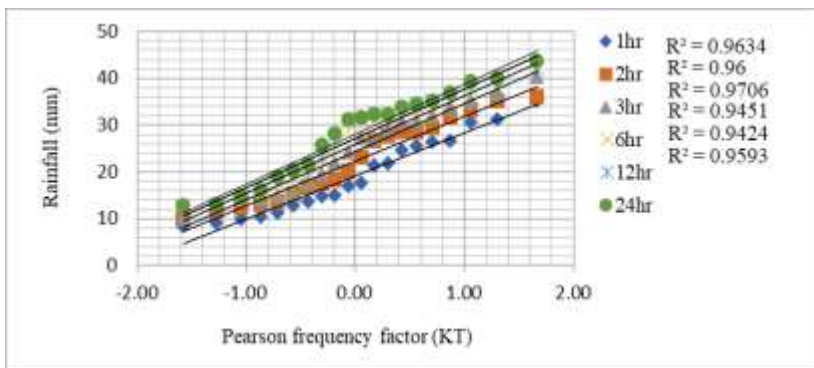
Appendix Figure 9. Plot of Pearson frequency factor against annual maximum rainfall for Log Pearson probability distribution for Mehal Meda station.